Theoretical study of short-range order in supercooled liquids and amorphous solids

Frank H. Stillinger and Leslie J. Root
AT&T Bell Laboratories, Murray Hill, New Jersey 07974

(Received 23 May 1988; accepted 30 June 1988)

The measurable properties of supercooled liquids and amorphous solids reflect the short-range packing geometry of the contituent particles. This paper is devoted to the description of that short-range order by the Born–Green–Yvon (BGY) local stress equation which relates pair and triplet distribution functions to the pair potential. Since metastable (but long-lived) phases are at issue, it has been necessary to identify an appropriate class of ensembles for which the BGY relation can be justified. In particular, low-temperature amorphous solids have preparation-method-dependent properties, and we propose to classify their representative ensembles by the choice of a triplet superposition correction function K. As background for such choice, we have reexamined and extended Alder's lattice enumeration method for K in regular structures. The Kirkwood superposition approximation $K \equiv 1$ has disastrous consequences for the BGY equation at low temperature; numerical pair correlation functions for the cases of hard spheres and of repelling Gaussian particles display long-range ordering that is impossible for the amorphous solid state. This failure is partially relieved by choosing a K that enhances the concentration of compact pentagonal particle groupings. Study of the inverse problem of determining K from physically reasonable pair correlation functions suggests that K must possess relatively long-ranged fluctuations about unity. These considerations highlight the desirability of accurate simulation studies of K for amorphous deposits at absolute zero.

I. INTRODUCTION

The scientific and technological need to understand atomic arrangements in noncrystalline materials continues to motivate sustained research effort. X-ray and neutron diffraction, Mössbauer spectroscopy, Rayleigh–Brillouin light scattering, and a wide variety of others experimental probes supply partial characterization of local order but leave many fundamental questions unanswered.[1–3] Recently computer simulation has begun to contribute insights into atomic order in glasses, but it suffers from restriction to very small systems, to short-time phenomena, and to relatively simple model Hamiltonians.[4–9]

The present paper is devoted to analytical and numerical study of short-range atomic (or molecular) order in low-temperature amorphous materials. These include supercooled liquids above their glass transitions, as well as amorphous solids at very low temperature; both are thermodynamically metastable states but display substantially time-independent properties. On account of the metastablity involved it is import to identify and to utilize the appropriate theoretical tools for their description.

Atomic distribution functions provide a compact and convenient description of short-range order. In the event that the material of interest comprises just one atomic species, the resulting single nth-order distribution function $\rho^{(n)}(\mathbf{r}_1 \cdots \mathbf{r}_n)$ is defined to give the density of n-tuplets of particles at locations $\mathbf{r}_1 \cdots \mathbf{r}_n$.[10] In the present cicumstances we can suppose that the system contains some large number N of identical particles, and is described by a time-independent normalized probability $P_N(\mathbf{r}_1 \cdots \mathbf{r}_N)$:

$$\int d\mathbf{r}_1 \cdots \int d\mathbf{r}_N \, P_N(\mathbf{r}_1 \cdots \mathbf{r}_N) = 1. \tag{1.1}$$

It may be assumed that P_N is invariant under permutation of the $\mathbf{r}_i$. This probability generates the $\rho^{(n)}$ as follows:

$$\rho^{(n)}(\mathbf{r}_1 \cdots \mathbf{r}_n) = [N!/(N-n)!] \times \int d\mathbf{r}_{n+1} \cdots \int d\mathbf{r}_N \, P_N(\mathbf{r}_1 \cdots \mathbf{r}_N). \tag{1.2}$$

Integration limits are provided by container wall positions for the system of interest.

The $\rho^{(n)}$ are expected to exhibit translational, rotational, and reflection symmetries within the interior of a bulk liquid, whether stable or supercooled. These symmetries *may* obtain for low-temperature amorphous solids, but exceptions should be expected. In particular, an amorphous solid deposit formed from the vapor by condensation on a cold substrate might grow in a somewhat anisotropic fashion, and that anisotropy could conceivably manifest itself in the $\rho^{(n)}$'s of all orders $n > 1$. Similarly, amorphous solids produced from crystals by damage from directed radiation beams might be strongly anisotropic.

Conventional classical statistical mechanics in the regime of thermal equilibrium takes P_N to represent an appropriate equilibrium ensemble. For the canonical ensemble at temperature $T = (k_B\beta)^{-1}$,

$$P_N = C(\beta) \exp[\beta\Phi(\mathbf{r}_1 \cdots \mathbf{r}_N)], \tag{1.3}$$

where Φ is the interaction potential and C is the normalization constant.[10,11] When $T > T_m$ (the melting temperature)

 0021-9606/88/205081-15$02.10

the $\rho^{(n)}$'s obtained from this canonical P_N are automatically those for the stable isotropic liquid. But as T declines below T_m this P_N yields the stable-crystal distribution functions.

The probability P_N clearly must be modified to yield $\rho^{(n)}$'s for the metastable supercooled liquid. An obvious strategy is to restrict the system configurations $\mathbf{r}_1 \cdots \mathbf{r}_N$ to amorphous structures, i.e., to set P_N to zero for those configurations expected to contribute to crystal-containing equilibrium states. A specific procedure for carrying out this restriction emerges from the "inherent structures" approach to condensed phase properties.[12,13] It is based upon a division of the full $3N$-dimensional configuration space into "basins," one for each local minimum of the potential energy Φ, followed by classification of those minima (mechanically stable particle packings) as "fully amorphous" vs "crystallite containing."[14,16] Let $\mathscr{R}_a$ represent the union of all basins for fully amorphous packings. The appropriate probability function for the supercooled liquid then is just an appropriately normalized canonical distribution over $\mathscr{R}_a$:

$$\begin{aligned} P_N(\mathbf{R}) &= C_a(\beta) \exp[-\beta\Phi(\mathbf{R})] \quad (\mathbf{R}\in\mathscr{R}_a) \\ &= 0 \qquad \text{(otherwise)}, \end{aligned} \tag{1.4}$$

where

$$1/C_a(\beta) = \int_{\mathscr{R}_a} d\mathbf{R} \exp[-\beta\Phi(\mathbf{R})], \tag{1.5}$$

and where $\mathbf{R} \equiv (\mathbf{r}_1,...,\mathbf{r}_N)$ is shorthand notation for the $3N$-dimensional system configuration vector. The choice (1.4) is consistent with the fact that reproducible measurements can be carried out on samples of supercooled liquids above their glass transition temperatures. Under this circumstance evidently the system is able to sample the amorphous region $\mathscr{R}_a$ with a sufficient approximation to ergodicity to justify use of a restricted canonical ensemble.

For real glass formers this situation no longer applies below the glass transition temperature. Exploration of the amorphous region $\mathscr{R}_a$ becomes too sluggish on the experimental time scale to justify use of Eq. (1.4). Instead the appropriate P_N and the various properties it implies become history dependent. Amorphous solids prepared by rapid and by slow cooling through the glass transition range, respectively, have measurably different characteristics, and would have to be represented by distinct P_N's. Low-temperature amorphous solids can be prepared by a variety of other techniques as well, including the abovementioned deposition from the vapor phase onto cold substrates,[17,18] high-dosage radiation damage to crystalline materials,[19,20] as well as mechanical disruption of crystals by high pressure.[21] In all such cases the appropriate P_N and the $\rho^{(n)}$'s obtained therefrom will depend on details of the method of preparation of the low-temperature amorphous material. It is physically reasonable to assume then that P_N is concentrated in a small subset of the Φ hypersurface basins, with only small vibrational excursions permitted from the respective potential energy minima.

With these general remarks as a background we proceed in Sec. II to examine the Born–Green–Yvon (BGY) intergrodifferential equation relating pair and triplet distribution functions $\rho^{(2)}$ and $\rho^{(3)}$. Our ultimate objective is to turn this local stress criterion into a means for predicting (or at least understanding) pair distribution functions in amorphous solids. This approach leads inevitably to reconsideration of the Kirkwood superposition approximation (Secs. II and III). Section IV presents results of some numerical analyses of the BGY equation which show that use of the Kirkwood superposition approximation leads to absurd predictions at low temperature; Sec. IV also shows that inclusion of certain types of short-range corrections to the Kirkwood approximation ameliorates but does not entirely eliminate that absurdity.

In order to develop an improved understanding of the role of corrections to the superposition approximation, we consider an "inverse problem" in Sec. V. This treats the amorphous solid pair distribution function at abolute zero temperature as given, and proceeds to extract the correction to the Kirkwood superposition approximation subject to a simple assumption about its functional form. The conclusions are, first, that the functional assumption utilized is appropriate for some, but not all, types of particle interactions; and second, that superposition corrections are at least a long ranged as the nontrivial part of the pair distribution function itself. In the light of this second conclusion we analyze in Sec. VI the large-distance asymptotic form of the BGY equation to obtain physically required conditions on the superposition correction.

Section VII summarizes our results and offers some suggestions for productive lines of future investigation.

II. BORN–GREEN–YVON EQUATION

For present purposes it is adequate to suppose that Φ is composed of central pair potentials:

$$\Phi(\mathbf{r}_1 \cdots \mathbf{r}_N) = \sum_{i<j=1}^{N} v(r_{ij}). \tag{2.1}$$

It has been demonstrated that amorphous particle packings indeed can exist in both two and three dimensions with a variety of pair potentials v.[12,22,23]

When the conventional canonical ensemble and its probability (1.3) are applicable, the following Born–Green–Yvon equation relating $\rho^{(2)}$ and $\rho^{(3)}$ can be straightforwardly derived:[10]

$$\begin{aligned} \nabla_1 \ln \rho^{(2)}(r_{12}) = &-\beta\nabla_1 v(r_{12}) - \beta \int d\mathbf{r}_3 [\nabla_1 v(r_{13})] \\ &\times \rho^{(3)}(r_{12},r_{13},r_{23})/\rho^{(2)}(r_{12}). \end{aligned} \tag{2.2}$$

Here it has been assumed that the system is very large and that container walls are sufficiently far from the region of interest to cause no direct effect. Furthermore, it has been supposed that the medium statistically is homogeneous and isotropic so that $\rho^{(2)}$ and $\rho^{(3)}$ at given temperature and density depend only on scalar distances.

It is convenient to introduce correlation functions $g^{(n)}$ in place of the $\rho^{(n)}$ by means of the definitions[10]

$$g^{(n)}(\mathbf{r}_1 \cdots \mathbf{r}_n) = \rho^{(n)}(\mathbf{r}_1 \cdots \mathbf{r}_N)/\rho^n, \tag{2.3}$$

where ρ is the particle number density N/V. As a consequence the BGY equation takes the form

$$\nabla_1 \ln g^{(2)}(r_{12}) = -\beta\nabla_1 v(r_{12}) - \beta\rho \int d\mathbf{r}_3[\nabla_1 v(r_{13})] \times g^{(3)}(r_{12},r_{13},r_{23})/g^{(2)}(r_{12}). \quad (2.4)$$

Aside from the factor β, the right-hand member of Eq. (2.4) represents the mean force experienced by particle 1 under the condition that particle 2 be located at a fixed distance r_{12}. This force consists of the direct force exerted on 1 by 2, as well as the average of the fluctuating net force on 1 due to all other surrounding particles in the system. If one designates the potential of mean force by $w(r_{12})$, then Eq. (2.4) is equivalent to the statement[10]

$$g^{(2)}(r_{12}) = \exp[-\beta w(r_{12})]. \quad (2.5)$$

It is generally believed that local order in liquids is short ranged. If the pair potential v decreases to zero exponentially with increasing distance, this can be taken to imply that $g^{(2)}(r_{12})$ approaches its large distance limit unity also with exponential decay.[24] The presence of long-range periodic order in three-dimensional crystals (even after orientational averaging) may produce a rather different behavior,[25–27] with $g^{(2)} - 1$ no longer exponentially decaying. Nevertheless, one still expects for the infinite system limit to find at positive temperature that

$$\lim_{r_{12}\to\infty} [g^{(2)}(r_{12}) - 1] = 0. \quad (2.6)$$

When the $3N$-dimensional probability density P_N has the restricted canonical form shown in Eq. (1.4), the BGY equation in principle exhibits a new term $\mathbf{A}_1$:

$$\nabla_1 \ln g^{(2)}(r_{12}) = \mathbf{A}_1(r_{12}) - \beta\nabla_1 v(r_{12}) - \beta\rho \int d\mathbf{r}_3[\nabla_1 v(r_{13})] \times g^{(3)}(r_{12},r_{13},r_{23})/g^{(2)}(r_{12}). \quad (2.7)$$

The vector $\mathbf{A}_1$ is a ratio of integrals:

$$\mathbf{A}_1(r_{12}) = \frac{\int_{\mathscr{S}_a(1,2)} \mathbf{D}_1(\mathbf{s}) \exp(-\beta\Phi)\, d\mathbf{s}}{\int_{\mathscr{R}_a(1,2)} \exp(-\beta\Phi)\, d\mathbf{r}_3 \cdots d\mathbf{r}_N}, \quad (2.8)$$

where $\mathscr{R}_a(1,2)$ is the portion $\mathscr{R}_a$ corresponding to fixed $\mathbf{r}_1$ and $\mathbf{r}_2$, $\mathscr{S}_a(1,2)$ is its boundary hypersurface, and $d\mathbf{s}$ is an element of hypersurface for $\mathscr{S}_a(1,2)$. The vector $\mathbf{D}_1$ measures the outward normal displacement of $\mathscr{S}_a(1,2)$ with respect to change in $\mathbf{r}_1$.

It is characterstic of good glass formers that their configuration points $(\mathbf{r}_1 \cdots \mathbf{r}_N)$ are virtually never to be found near the boundary of $\mathscr{R}_a$, for otherwise the rate of crystal nucleation would be high. Consequently we are justified in setting $\mathbf{A}_1$ equal to zero in Eq. (2.7), thereby causing the equation to reduce precisely to the conventional BGY equation (2.4).

In the case of amorphous solids at absolute zero, every particle experiences vanishing net force. That is, the appropriate ensemble comprises a collection of particle configurations all of which corespond to mechanically stable packings (potential minima). In this case we can finally write the following conditions:

$$0 = \nabla_1 v(r_{12}) + \rho \int d\mathbf{r}_3[\nabla_1 v(r_{13})] g^{(3)}(r_{12},r_{13},r_{23})/g^{(2)}(r_{12}), \quad (2.9)$$

where $g^{(2)}$ and $g^{(3)}$ are the correlation functions for the $T = 0$ amorphous medium. This is the pair-space force balance condition, stating that the direct force on particle 1 due to a specific neighbor 2 must be exactly compensated by the net force due to all others in the vicinity. Notice that aside from a missing factor β the right member of Eq. (29) is precisely the same as the right member of the conventional BGY equation (2.4). Since β diverges to infinity as temperature declines to absolute zero, force balance equation (2.9) would automatically have to be satisfied by the $T\to 0$ solutions to the BGY equation, provided $\nabla_1 \ln g^{(2)}$ remained bounded. This last condition evidently is satisfied by pair correlation functions for amorphous solids.[1,28,29] In view of these observations it seems attractive to try to solve the BGY equation over the entire temperature range from above the thermodynamic melting point down to absolute zero as a means for predicting amorphous-solid pair correlation functions. Implementing such a program requires a closure relation to specify the triplet function $g^{(3)}$. Quite generally for isotropic and homogeneous media (and specifically solid amorphous media) we can write

$$g^{(3)}(r_{12},r_{13},r_{23}) = g^{(2)}(r_{12})g^{(2)}(r_{13})g^{(2)}(r_{23}) \times K(r_{12},r_{13},r_{23}), \quad (2.10)$$

where the nonnegative function K is symmetric in its three spatial variables, and approaches unity as any one of the three particles recedes from the other two. The most widely used closure is the Kirkwood superposition approximation:[10,30]

$$K(r_{12},r_{13},r_{23}) \cong 1; \quad (2.11)$$

in the case of fluids in the high-temperature equilibrium regime the BGY equation with this approximation leads to qualitatively reasonable estimates of $g^{(2)}$.[31] However, we shall see below that this closure is not appropriate for low-temperature amorphous solids. It should be noted in passing that several proposals have been advanced for improvement to the Kirkwood superposition approximation for $g^{(3)}$.[32,33]

In the following we take the point of view that amorphous states of a given substance can be classified by the corresponding K's, and that distinct preparation methods each correspond to some specific K. By choosing the correct K for insertion into the BGY equation it becomes possible in principle to see how $g^{(2)}$'s are affected by preparation method.

III. LATTICE COMBINATORICS

No experimental technique is available for complete determination of the triplet correlation function $g^{(3)}$. Fortunately computer simulation is nowadays able to determine the function at least partially for some simple models. Results have been published for hard spheres,[34] for the model with Lennard-Jones interactions,[35–38] and for a model of liquid sodium.[39] In each of these cases, $K(r_{12},r_{13},r_{23})$ displays significant deviations from unity for thermodynamically sta-

ble fluid states, strongly suggesting that deviations of at least comparable magnitude should be expected in low-temperature amorphous states.

At least for simple atomic substances the short-range order in amorphous packings appears to resemble that of the corresponding stable crystalline form.[22,28,40] For that reason it is relevant to present interests to examine the superposition correction function K for fully ordered crystal structures. Alder[34] has pointed out that this can be done by straightforward lattice enumeration. In this section we revisit the Alder method, providing an extension, a correction, and some interpretation.

At the pair correlation function level, spherically averaged short-range order can be specified by giving coordination numbers Z_ν and coordination radii R_ν for each of the successive shells of neighbors ($\nu = 1,2,...$); tabulations of these parameters are available.[41] The corresponding representation for the pair correlation function is[42]

$$g^{(2)}(r) = (4\pi\rho)^{-1} \sum_{\nu=1}^{\infty} Z_\nu R_\nu^{-2} \delta(r - R_\nu). \tag{3.1}$$

In a macroscopically large portion of the crystal containing N atoms the expected number of pairs at distance R_ν is $Z_\nu N/2$.

For triads of distance R_λ, R_μ, R_ν out of which a triangle can be formed (including a zero-area degenerate triangle), $K(R_\lambda,R_\mu,R_\nu)$ can be calculated by comparing the actual enumeration of such triangles in the lattice with the number implied by the Kirkwood superposition approximation. Denote the actual number in an N-atom macroscopic crystal by $\omega(R_\lambda,R_\mu,R_\nu)N$. The superposition estimate is easily found for nondegenerate triangles as follows:

$$\begin{aligned}&\sigma^{-1} V \int_{R_\lambda-\epsilon}^{R_\lambda+\epsilon} 4\pi r^2\, dr (2\pi/r) \\ &\times \int_{R_\mu-\epsilon}^{R_\mu+\epsilon} s\, ds \int_{R_\nu-\epsilon}^{R_\nu+\epsilon} t\, dt\, \rho^3 g^{(2)}(r) g^{(2)}(s) g^{(2)}(t) \\ &= V Z_\lambda Z_\mu Z_\nu (8\pi R_\lambda R_\mu R_\nu \sigma)^{-1},\end{aligned} \tag{3.2}$$

where V is N/ρ, the sample volume, σ is a symmmetry factor for the triangle (1, 2, or 6 for scalene, isoceles, or equilateral), and we have used bipolar coordinates to carry out the inner integrals. Consequently we have the following result for nondegenerate triangles:

$$\begin{aligned}K(R_\lambda,R_\mu,R_\nu) &= 8\pi\rho\sigma R_\lambda R_\mu R_\nu (Z_\lambda Z_\mu Z_\nu)^{-1} \\ &\times \omega(R_\lambda,R_\mu,R_\nu).\end{aligned} \tag{3.3}$$

The degenerate triangle case, wherein one of the three distances equals the sum of the other two, requires special attention. An easy route to the correct result for the superposition estimate temporarily first replaces the Dirac delta functions in Eq. (3.1) by positive-width normalized distributions, e.g.,

$$\begin{aligned}\Delta(x) &= (2\epsilon)^{-1} \quad (|x| \leqslant \epsilon) \\ &= 0 \qquad (\epsilon < |x|).\end{aligned} \tag{3.4}$$

The necessary integrals can be carried out for positive ϵ, and then ϵ allowed to go to zero in the result. This yields finally

TABLE I. Nonvanishing superposition correction factors for the face-centered-cubic lattice.

r^2	s^2	t^2	$K(r,s,t)$
1	1	1	0.987 307
1	1	2	1.396 263
1	1	3	0.855 033
1	1	4	0.987 307
1	2	3	1.209 200
1	2	5	1.561 070
1	3	3	0.740 481
1	3	4	1.710 066
1	3	5	0.955 956
1	4	5	1.103 843
1	5	5	1.234 134
2	2	4	7.898 459
2	3	3	2.094 395
2	5	5	1.745 329
3	3	3	0.641 275
3	3	4	0.740 481
3	3	5	1.655 765
3	4	5	1.911 912
4	4	4	7.898 459
4	5	5	1.234 134

$$\begin{aligned}K(R_\lambda,R_\mu,R_\nu) &= 16\pi\rho\sigma R_\lambda R_\mu R_\nu (Z_\lambda Z_\mu Z_\nu)^{-1} \\ &\times \omega(R_\lambda,R_\mu,R_\nu) \quad \text{(deg triangles)}.\end{aligned} \tag{3.5}$$

Notice that the form obtained is larger by a factor 2 than that in Eq. (3.3) for nondegenerate triangles.

We have made extensive tabulations of K's for both the face-centered-cubic (fcc) and the body-centered-cubic (bcc) lattices, utilizing a digital computer to effect the necessary enumerations for ω. Tables I and II present a few of our results. The K values are independent of density for these perfect lattices, and for notational simplicity in both tables we have taken the nearest-neighbor separation to be unity ($R_1 = 1$).

Alder was concerned only with the face-centered-cubic lattice.[34] Our results in Table I agree with his except for the degenerate triangle R_1, R_1, R_4.

TABLE II. Nonvanishing superposition correction factors for the body-centered-cubic lattice.

r^2	s^2	t^2	$K(r,s,t)$
1	1	4/3	2.356 195
1	1	8/3	1.666 081
1	1	4	2.040 524
1	4/3	11/3	1.503 923
1	8/3	11/3	2.126 868
1	11/3	4	1.953 653
1	11/3	16/3	3.007 846
4/3	4/3	8/3	3.949 229
4/3	4/3	16/3	5.585 054
4/3	8/3	4	5.130 199
4/3	11/3	11/3	1.919 862
8/3	8/3	8/3	3.949 229
8/3	8/3	16/3	5.585 054
8/3	11/3	11/3	2.036 321
11/3	11/3	4	2.493 974
4	4	16/3	18.849 556

The lattice K's display remarkable deviations from unity for many triangles in both the fcc and bcc cases. There are examples where K vanishes identically; the periodic lattice structures prohibit formation of triangles from some distance triads. Contrariwise, K occasionally becomes very large indeed, as in the following fcc example:

$$K(R_8,R_8,R_{16}) = 63.187\,67. \tag{3.6}$$

We conjecture that arbitrarily large K's exist for triangles of unbounded size.

It may be worth pointing out that this method of obtaining K can easily be generalized to lattices with vacancies, provided no distortion around those vacancies is involved. A strictly random vacancy distribution would cause no change in the K's. However, various nonrandom distributions could be created which would significantly change those initially nonvanishing K's.

Lattice enumeration only estimates K for a discrete set of configurations. To the extent that amorphous packings contain defective but identifiable order of the type present in some perfect lattice, the enumeration results may indeed be qualitatively relevant for amorphous materials. It is worth pointing out that some evidence for this point of view emerges from the computer simulations of Lennard-Jones liquids, for which the crystalline phase is close packed (fcc or hcp depending on the potential cutoff used). For those configurations close to the isosceles triangle, R_1, R_2, R_2 which Table I shows to be missing in the fcc crystal, the liquid simulation K tends to be anomalously low compared to the superposition value unity.[38] By contrast, configurations in the liquid near R_1, R_1, R_2 have K significantly greater than unity,[38] consistent with the corresponding entry in Table I. Recall that the inherent structure theory for liquids[12,13] interprets these as vibrationally smeared versions of those for certain static amorphous packings.

In very broad terms it becomes clear from the Alder lattice enumeration approach that the superposition correction factor K is a sensitive indicator of geometric order. How important this is for numerical solutions of the BGY equation emerges clearly in Sec. IV.

IV. DIRECT NUMERICAL INTEGRATIONS

The BGY vector Eq. (2.4) can be reduced to scalar form by employing bipolar coordinates:

$$\begin{aligned} -[\beta g(r_{12})]^{-1}g'(r_{12}) &= v'(r_{12}) + \pi\rho r_{12}^{-2}\int_0^\infty dr_{13}\, v'(r_{13})g(r_{13}) \\ &\times\int_{|r_{12}-r_{13}|}^{r_{12}+r_{13}} dr_{23}\, r_{23}(r_{12}^2 + r_{13}^2 - r_{23}^2)g(r_{23}) \\ &\times K(r_{12},r_{13},r_{23}). \end{aligned} \tag{4.1}$$

For notational simplicity we have set $g^{(2)}\equiv g$. After invoking the Kirkwood superposition approximation (2.11), the resulting nonlinear integrodifferential equation can be used to predict g, and several numerical studies of this kind at positive temperature have been published.[43–49] As marked in Sec. II, amorphous solids at absolute zero are described by Eq. (4.1) with the left member set to zero.

In this section we report some numerical solutions for Eq. (4.1) first with $K = 1$, and then with some physically motivated choices for K that incorporate significant deviations from unity.

A. Hard spheres

After setting $K = 1$, the absolute zero form of Eq. (4.1) is

$$\begin{aligned} 0 &= v'(r_{12}) + \pi\rho r_{12}^{-2}\int_0^\infty dr_{13}\, v'(r_{13})g(r_{13}) \\ &\times\int_{|r_{12}-r_{13}|}^{r_{12}+r_{13}} dr_{23}\, r_{23}(r_{12}^2 + r_{13}^2 - r_{23}^2)g(r_{23}). \end{aligned} \tag{4.2}$$

The hard-sphere pair interaction $v_{\rm HS}$ may be regarded as the limit of a sequence of continuous potentials, e.g.,

$$\begin{aligned} v_{\rm HS}(r) &= \lim_{n\to\infty} r^{-n} \\ &= +\infty \quad (0\leqslant r<1) \\ &= 0 \quad (1<r). \end{aligned} \tag{4.3}$$

For simplicity the hard-sphere collision diameter has been set to unity. The product $v'g$ can only be nonvanishing at the collision diameter, and so will be proportional to a Dirac delta function:[50]

$$v'(r)g(r) = -C_0\delta(r-1). \tag{4.4}$$

Consequently, when $r_{12}>1$ we see that Eq. (4.2) reduces to the following:

$$0 = \int_{r_{12}-1}^{r_{12}+1} dr_{23}\, r_{23}(r_{12}^2 + 1 - r_{23}^2)g(r_{23}) \quad (r_{12}>1). \tag{4.5}$$

Notice that the unknown constant C_0 from Eq. (4.4) has conveniently vanished. By setting

$$\psi(y) = y[g(y) - 1] \tag{4.6}$$

it is easy to see that integral Eq. (4.5) is equivalent to

$$0 = \int_{x-1}^{x+1}(x^2 + 1 - y^2)\psi(y)dy \quad (x>1). \tag{4.7}$$

As it stands, Eq. (4.7) cannot uniquely determine ψ. It is a homogeneous equation and leaves ψ at least undetermined as regards a multiplicative constant. But in view of the absolute exclusion of hard-sphere pairs closer than the collision diameter, we must observe the following accessory condition:

$$\psi(y) = -y \quad (0\leqslant y<1). \tag{4.8}$$

This should help to determine ψ uniquely.

If the restriction $x>1$ is removed from Eq. (4.7), ψ can formally be defined on the negative real axis so as to satisfy that equation for all x. By applying two x derivatives, Eq. (4.7) then converts to a linear and homogeneous differential-difference form:

$$0 = \psi'(x+1) + \psi'(x-1) - \psi(x+1) + \psi(x-1). \tag{4.9}$$

This formally has as its solutions linear combinations of complex exponentials:

$$\psi(x) = \sum_j A_j \exp(ik_j x) \tag{4.10}$$

provided that each k_j is a root of the transcendental equation

$$k = \tan k. \tag{4.11}$$

One easily verifies that each complex exponential individually satisfies the integral Eq. (4.7) over the entire real axis. The coefficients A_j must be selected to assure that accessory condition (4.8) is satisfied as well.

It is relatively easy to show that Eq. (4.11) has only real roots, that they are infinite in number, and occur as pairs $\pm |k_j|$. The origin $k = 0$ is a triple root, and as a consequence arbitrary quadratic functions of x satisfy Eqs. (4.7) and (4.9); however, on physical grounds we can eliminate them from further consideration. Thus we need to consider only nonvanishing k_j's.

The roots k_j are relatively easy to compute to high precision. As becomes obvious from a graphical analysis of Eq. (4.11), the k_j approach equal spacing far from the origin. One can show that their asymptotic locations are given by

$$|k_n| = (n - \tfrac{1}{2})\pi - [(n - \tfrac{1}{2})\pi]^{-1} - 2[3(n - \tfrac{1}{2})^3\pi^3]^{-1} + \cdots \tag{4.12}$$

for large positive integers n.

After restricting attention to the first 200 nonvanishing k_j's nearest the origin for numerical feasibility, we have evaluated the corresponding A_j's by requiring condition (4.8) to be satisfied at 200 equally spaced points along $0 \leqslant y < 1$. This fully determines ψ (and thus g), subject to the truncated set of k_j's utilized. Figure 1 exhibits the resulting pair correlation function $g(x)$. This result appears to exhibit jump discontinuities whenever x is a positive integer, through their magnitudes seem to decline as distance increases. The "fuzziness" shown by the solution in every other interval results from rapid oscillations due to high-order k_j's. Our systematic studies indicate that as more and more roots are included the amplitude of the fuzziness declines to leave a smooth function located near the middle of the oscillation endpoints.

This numerical solution has several physically unacceptable characteristics which constitute a serious challenge to the superposition approximation for hard spheres. First, the solution is independent of number density ρ, whereas one expects mechanically stable random packings of spheres to show a rather narrow range of densities.[51] Second, it is normally expected that random hard-sphere packings should exhibit contact Dirac delta functions (each particle jammed by at least four others),[22] whereas none appears in the superposition solution. Third, it is difficult to imagine credible geometric circumstances that would produce an infinte sequence of jump discontinuities in g at every positive integer multiple of the collision diameter.

B. Gaussion core model

The physical deficiencies just noted for g in Fig. 1 might conceivably be attributable to the peculiar singular nature of the hard-sphere interaction. For that reason we have investigated the contrasting case where particles interact in pairs with a Gaussian potential:

$$v(r) = \epsilon \exp[-(r/\sigma)^2]; \tag{4.13}$$

in the following we take $\epsilon = \sigma = 1$. A substantial body of analytical work[52–55] and molecular dynamics computer simulation[56–61] is available for this Gaussian core model. In particular it has been determined that the model produces mechanically stable amorphous packings.[57]

We chose to solve the BGY equation with the superposi-

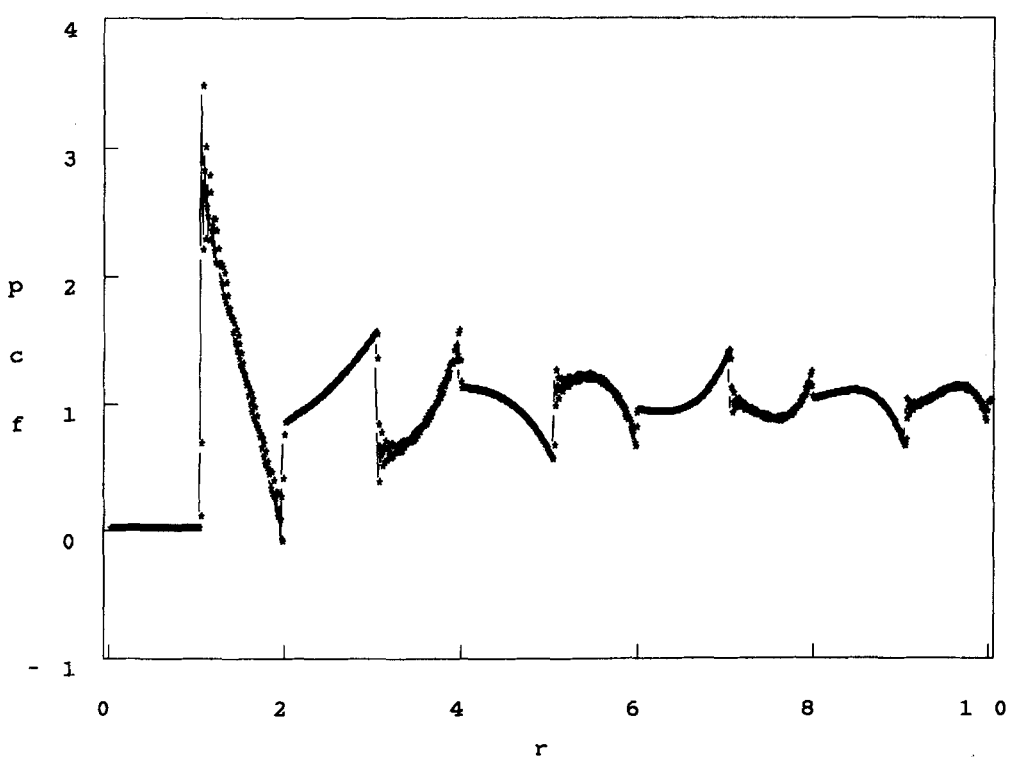

FIG. 1. Numerical pair correlation function for the BGY superposition equation, intended to describe the $T = 0$ amorphous state for hard spheres.

tion approximation for the Gaussian core model first at high temperature. The temperature was then lowered in stages (using a preceding higher temperature solution as starting point) in the hope that a realistic limiting pair correlation function for absolute zero could ultimately be obtained.

For numerical purposes it is convenient to use the integrodifferential equation in the following form integrated over variable r_{12} [10]:

$$\beta^{-1} \ln g(r_{12}) = -\exp(-r_{12}^2) + 2\pi\rho r_{12}^{-1} \times \int_0^\infty dr_{23}\, L(r_{12},r_{23})[g(r_{23}) - 1], \tag{4.14}$$

where the kernel L is

$$L = r_{23} \int_{|r_{12}-r_{23}|}^{r_{12}+r_{23}} dr_{13}\, r_{13}[(r_{12}-r_{23})^2 - r_{13}^2] \times \exp(-r_{13}^2) g(r_{13}). \tag{4.15}$$

Owing to the short-range nature of the Gaussian potential, L becomes negligibly small unless r_{12} and r_{23} are comparable. Solutions to Eqs. (4.14) and (4.15) were obtained by iteration, with suitable mixing of present and previous iterates.[33]

Figure 2 presents a pair correlation function at relatively high temperature ($\beta^{-1} = k_B T = 0.05$), where the number density $\rho = 0.1$. Although the pair interaction is bounded for all r, its small-distance repulsion has effectively prevented pairs from approaching more closely than $r \cong 1$. Beyond this repulsive core region the indicated short-range order in the fluid is quite weak.

Reduction in temperature enhances the range and magnitude of short-range order. Figure 3 shows the pair correlation function at the same density, but with $\beta^{-1} = k_B T = 0.008\,82$. Results obtained between the temperatures of Figs. 2 and 3 illustrate smooth and continuous change.

Small further reduction in temperature below 0.008 82 induces a discontinuous change in g. Figure 4 shows the result at $\beta^{-1} = 0.008\,78$, $\rho = 0.1$. The numerical solution suddenly has developed a regular train of pulses. The upper cutoff used was $r = 50$; our studies indicate that increasing the cutoff simply extends the pulse sequence which in the limit of infinite cutoff approaches a periodic sequence. Similar pulse-train solutions to the superposition BGY equation have been reported previously for the square-well and hard-sphere models by Co, Kozak, and Luks.[48,49,62]

At even lower temperatures the pulse-train type of solution remains, but with higher and narrower pulses which makes the numerical analysis increasingly difficult. Figure 5 shows the computed pair correlation function at $\beta^{-1} = 0.004$, $\rho = 0.1$. Notice that the separation between pulses is virtually unchanged.

So far as we have been able to establish there is no temperature range over which both types of solutions simultaneously exist.

It seems clear that upon approaching absolute zero the only solution to the superposition BGY equation will involve a regularly spaced sequence of Dirac delta functions. No spatial arrangement of particles in three dimensions can produce pair correlation functions of this type, or for that matter the positive-temperature types shown in Figs. 4 and 5. Obviously the Kirkwood superposition approximation has created another dramatic failure.

We have also examined numerical solutions to the superposition BGY equation for the Gaussian core model at the higher density $\rho = 1.0$. The situation is qualitatively the same, with smooth and damped g at high temperature, but

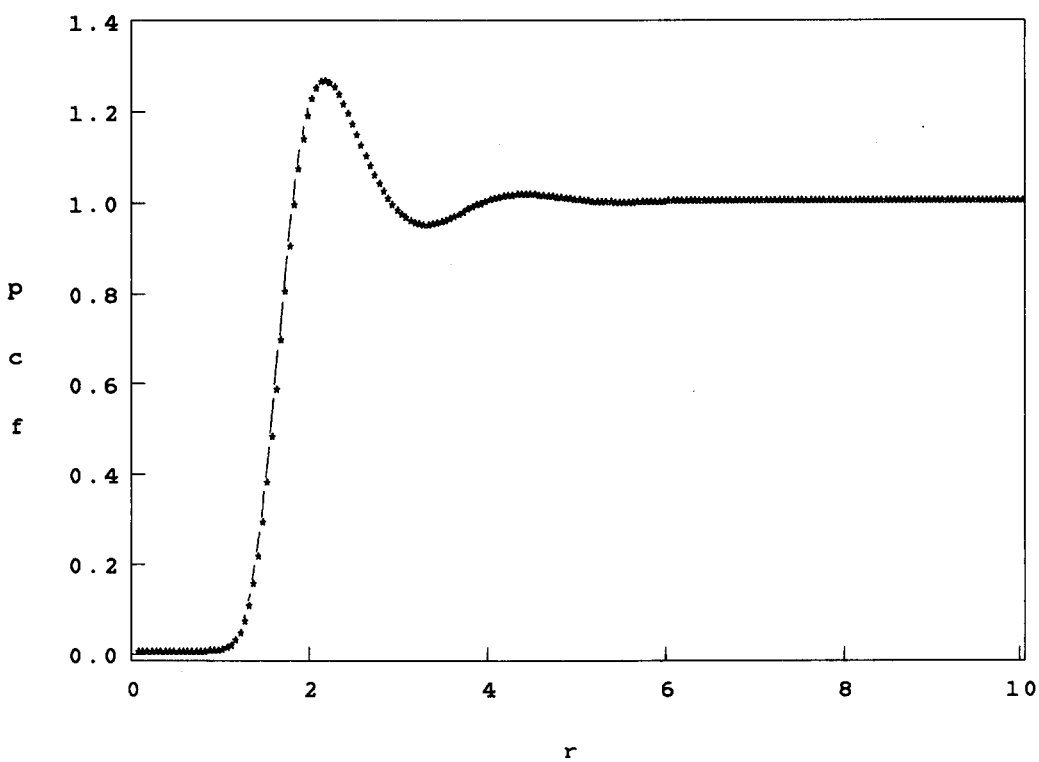

FIG. 2. Pair correlation function for the Gaussian core model at $\beta^{-1} = 0.05$, $\rho = 0.1$ obtained from numerically integrating the BGY equation with the superposition approximation.

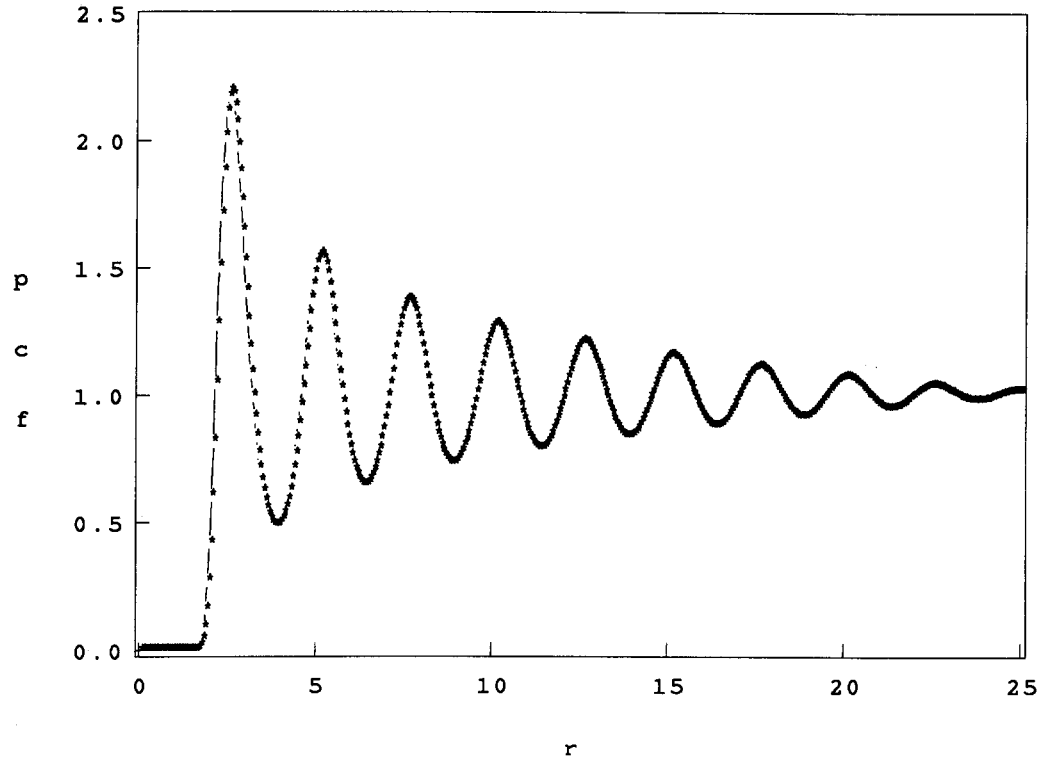

FIG. 3. Pair correlation function for the Gaussian core model at $\beta^{-1} = 0.008\,82$, $\rho = 0.1$, from the BGY equation with the Kirkwood superposition approximation.

pulse-train solutions at low temperature. The discontinuous change from one type to the other occurs near $\beta^{-1} = 0.1$, and the separation between successive pulses is less than at $\rho = 0.1$ (but not as much less as simple $\rho^{-1/3}$ distance scaling would imply).

As further measures of physical inappropriateness of the pulse-train solutions, we mention that the mean potential energy and the virial pressure implied by those solutions suddenly rise as temperature declines through the discontinuity point.

C. Short-range superposition corrections

The failure of the preceding attempts to construct reasonable zero-temperature amorphous-state pair correlation functions for the hard-sphere and Gaussian core models dra-

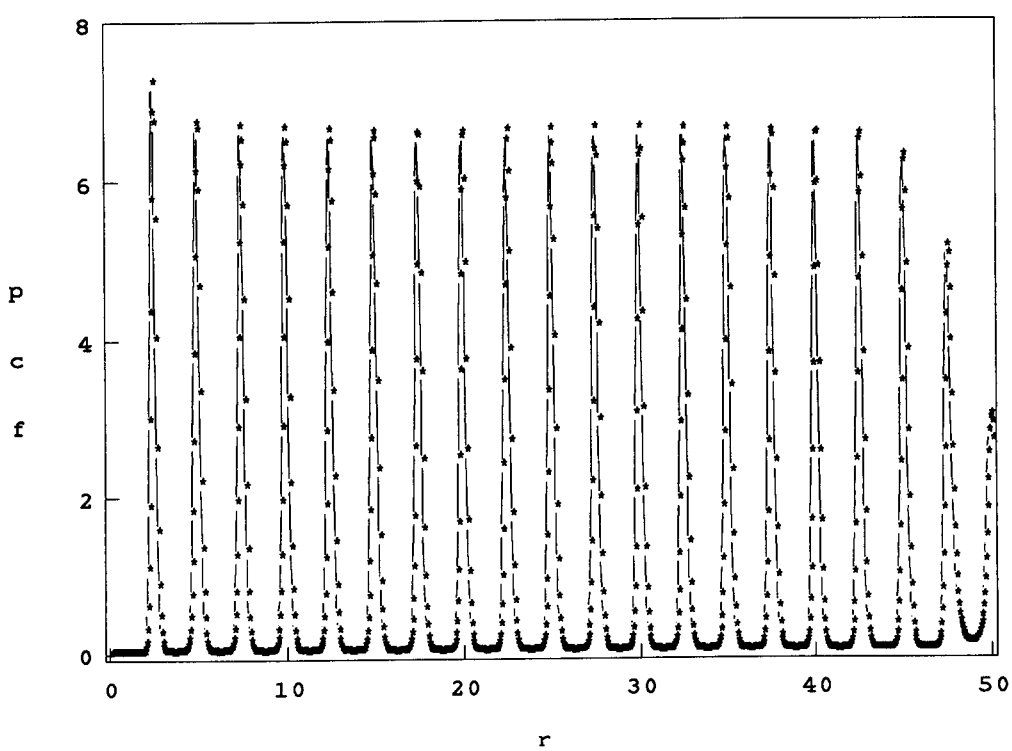

FIG. 4. Pair correlation function for the Gaussian core model at $\beta^{-1} = 0.008\,78$, $\rho = 0.1$, from the BGY equation with the superposition approximation.

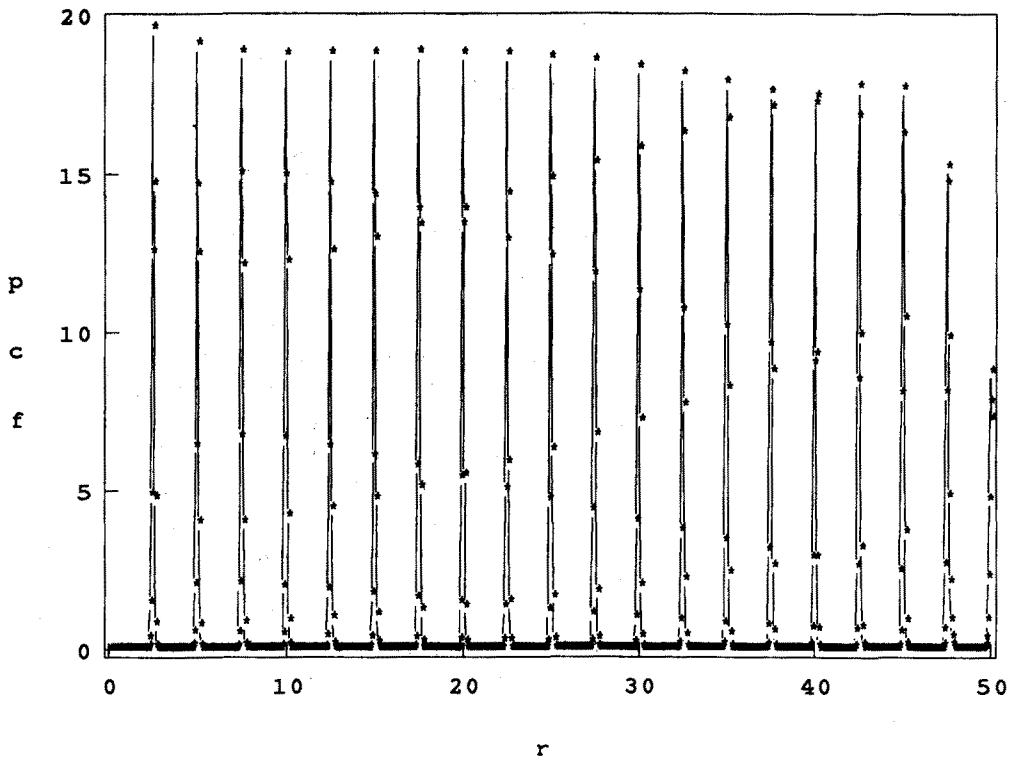

FIG. 5. Pair correlation function for the Gaussian core model at $\beta^{-1}=0.004$, $\rho=0.1$, from the BGY equation with the superposition approximation.

matizes the importance of correction to the Kirkwood superposition approximation. We now describe the effects of an attempt to correct the superposition approximation for some compact arrangements of three particles.

If we trivially rewrite K thus:

$$K(r,s,t)=1+D(r,s,t), \tag{4.16}$$

then we know that in the amorphous solid state the superposition deviation function D must vanish in the limit that at least two of its variables become infinite. We shall tentatively assume that D can be approximated in the following way:

$$D(r,s,t)\cong\sum_j A_j f(a_j\Delta_j); \tag{4.17}$$

$$\Delta_j^2=(r-r_j)^2+(s-s_j)^2+(t-t_j)^2; \tag{4.18}$$

$$f(x)=(1-x^2)^2 \quad (|x|<1)$$
$$=0 \quad (|x|\geqslant 1). \tag{4.19}$$

The index j covers a finite selection of relevant triangles (sides r_j,s_j,t_j) where occurrence probabilities can be enhanced or inhibited according as the constants A_j are positive or negative, respectively. The positive width constant a_j controls how much distortion any selected triangle can undergo before its contribution to D disappears. Since D must be fully symmetric in r, s, and t the j sum in Eq. (4.17) must include all relevant triangle side permutations.

At this stage the lattice enumerations presened in Sec. III above become relevant. Since there is reason to suspect that amorphous solids contain a substantial proportion of local particle arrangements similar to those in the stable crystal,[22,28,40] it seems appropriate to craft the expression (4.17) accordingly.

The stable crystal form for the Gaussian core model at density 0.1 is face centered cubic, while at the higher density 1.0 it is body centered cubic.[52,54] Results in Tables I and II suggest that among the small triangles the strongest deviations from superposition are associated with totally missing triangles. These are the cases (1,2,2) for fcc, and (1,1,1) for bcc.

The BGY equation has been iteratively solved for the Gaussian core model at $\rho=0.1$ with a symmetric three-term approximation for D that is intended partially to inhibit the characteristic (1,2,2) triangles. We chose the following values for the stength and width parameters:

$$A_j=-0.5023,$$
$$a_j=0.8270. \tag{4.20}$$

The resulting pair correlation functions resembled those with the superposition approximation, for $\beta^{-1}>0.015$. However, no convergence to a fluid or amorphous solid $g(r)$ was obtained at lower temperature. Even the pulse-train solutions were not obtained, but only artifactual solutions with unphysical wide oscillations between successive numerical grid points. The choice (4.20) has made the situation even worse than before.

For the $\rho=1.0$ case, D is taken to be a single term corresponding to the manifestly symmetric equilaterial triangle of nearest neighbors. The strength and width constants were selected to be

$$A_j=-0.495\,38,$$
$$a_j=1.7818 \text{ and } 3.5636, \tag{4.21}$$

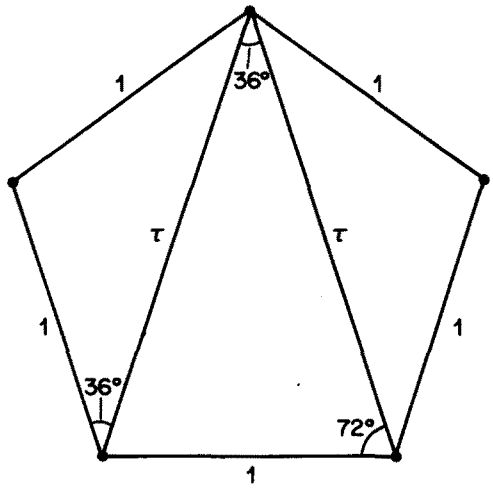

FIG. 6. Particle triangles comprised in regular pentagonal structures. The length τ is the golden mean $(5^{1/2}+1)/2$.

where the latter two alternatives were examined in turn to observe the effects of width change. The numerical study uncovers results that at best are marginally changed from the superposition approximation, namely fluid-like solutions (broad and damped features) for temperatures above 0.09, and pulse-train solutions below.

Finally we adopted the suggestion that pentagonal units play an important role in supercooled liquids and amorphous solids.[63–65] For the Gaussian core model at $\rho = 0.1$ we therefore integrated the BGY equation with D chosen to enhance the two types of isosceles triangles that occur within regular pentagons. These are illustrated in Fig. 6. Following earlier notation (Tables I and II) these triangles would be denoted by $(1,1,\tau^2)$ and $(1,\tau^2,\tau^2)$ where the nearest-neighbor distance is that for the fcc lattice at the given density, and

$$\tau = (5^{1/2}+1)/2 = 1.618\,03\cdots \tag{4.22}$$

is the famous "golden mean." Six terms are required for D (three for each type of triangle). The strength and width parameters were taken to be the same for both types:

$$A_j = 3.0000,$$
$$a_j = 1.0338. \tag{4.23}$$

The resulting numerical study of the BGY equation with these pentagonal enhancements showed that the physically acceptable $g(r)$ solutions with damped short-range order extended to much lower temperature than with no such enhancements (i.e., the superposition approximation). Figure 7 shows such a solution at $\beta^{-1} = 0.0004$, $\rho = 1.0$. Further lowering of temperature appears to eliminate this "physical" solution branch however. Although limited computing resources prevented complete study of this lower temperature region, partial results seem to suggest that the very slowly converging iterations would produce pulse-train solutions as before.

Consequently, pentagonal enhancements are beneficial to the extent of lowering by roughly a factor 20 the minimum temperature at which physical $g(r)$ solutions could be obtained (from 0.008 78 to 0.0004). However these acceptable solutions could still not be extended to aboslute zero as required.

V. INVERSE PROBLEM

An independent source of information about the role of triplet correlations in amorphous solids arises by turning the

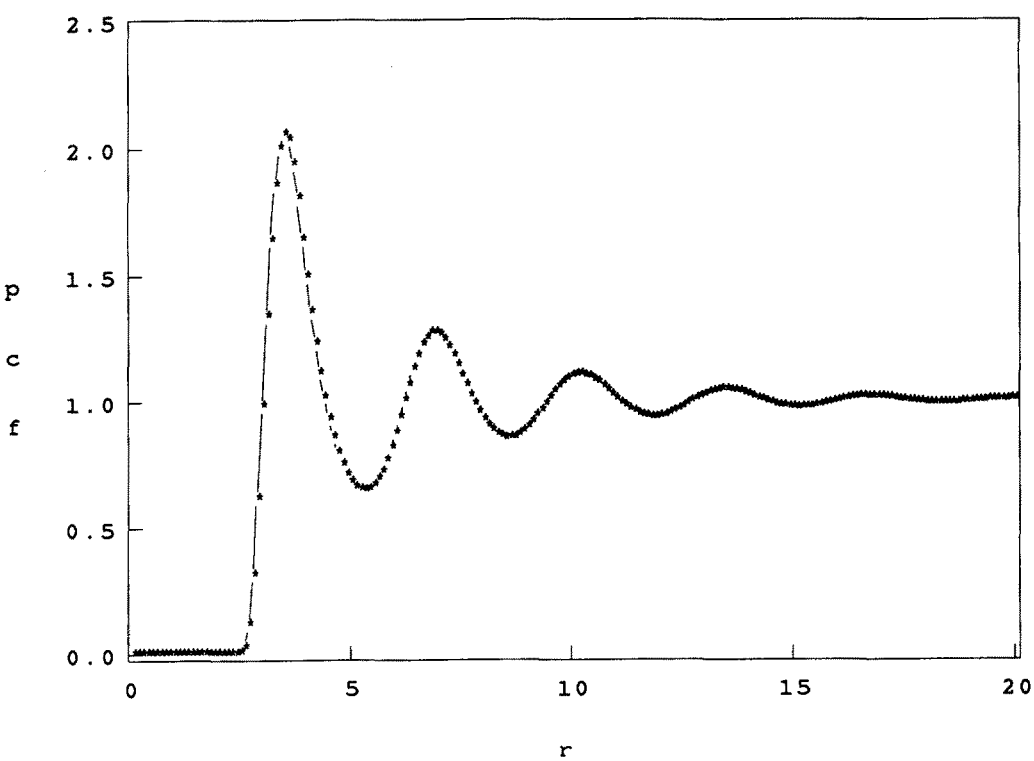

FIG. 7. Pair correlation function for the Gaussian core model at $\beta^{-1} = 0.0004$, $\rho = 1.0$. This was obtained by solving the BGY equation with corrections to the superposition approximation that enhance pentagonal packing structures [Eqs. (4.22) and (4.23)].

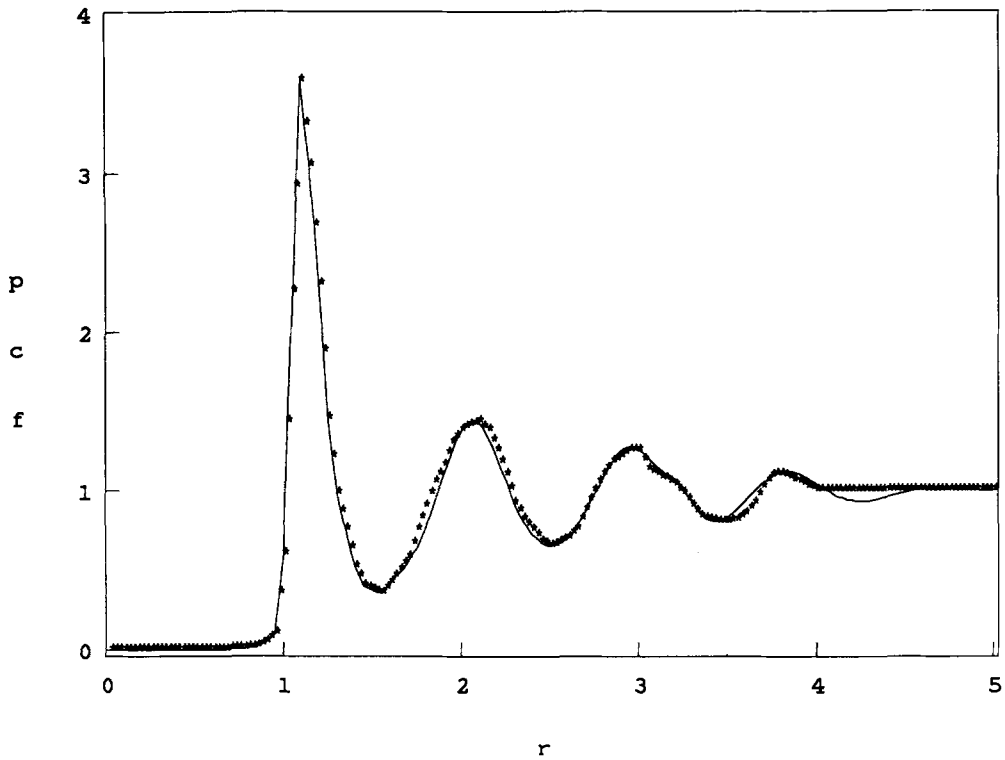

FIG. 8. Amorphous-state pair correlation function for the $\rho = 1.0$ Gaussian core model calculations of Ref. 57 (asterisks). The solid curve is an analytic fit function.

problem around. Specifically, we can ask what form must the function K have in order to be consistent with a given $g(r)$ for an amorphous solid. The latter can be taken from computer simulation for models with simple pair potentials. Attention will be confined to the zero-temperature limit.

In order to have a mathematically well-posed problem with an unique solution it is necessary to restict K somewhat. In particular we have tentatively assumed that K depends on a single spatial variable that preserves the basic r, s, t symmetry, namely,

$$K(r,s,t) \equiv K(r+s+t). \tag{5.1}$$

Consequently the zero-temperature BGY equation (2.9) adopts the following form:

$$0 = v'(r) + \pi\rho r^{-2} \int_0^\infty ds \int_{|r-s|}^{r+s} dt\, v'(s) t (r^2 + s^2 - t^2) \times g(s) g(t) K(r+s+t). \tag{5.2}$$

After discretizing the distance variables by constant subdivision out to a suitable upper limit, and then approximating the integrals by sums, Eq. (5.2) becomes a set of linear equations for the K values. The solution then can be obtained by standard procedures.

We have examined two cases for which $T = 0$ amorphous-state pair correlation functions were available to us in tabular form, namely the Gaussian core model,[57] and the "v_5" model whose pair potential approximates the behavior of noble gas atoms.[29]

Figure 8 shows (asterisks) the Gaussian core model input data. This represents the pair correlation function at $\rho = 1.0$ for a single stable packing of 432 particles with periodic boundary conditions, prepared by slow cooling (without crystal nucleation) from the liquid phase. Since this one sample contains substantial statistical uncertainty, we were motivated to smooth the data with an analytical fit function; the fit appears as a solid curve in Fig. 8. Considering the small system size and very limited sampling of packings, we regard the fit as reasonable.

Figure 9 shows the resulting $K(r+s+t)$ from the inversion procedure that incorporates the smoothed data of Fig. 8. Several observations are warranted. First, K is nonnegative as we know it must be, and it approaches unity at large values of the perimetric variable $u = r+s+t$. Second, it is really not possible to determine K for u smaller than about 2.5 simply because the input data effectively contains no contributions from triangles of such small perimeters. Third, this K implies very substantial corrections to the superposition approximation for compact triangles. Fourth and most important, the deviations of K from unity have a spatial range that is at least as great as that of g itself.

The dimensionless v_5 potential has the following specific form:

$$\begin{aligned} v_5(r) &= B(r^{-12} - r^{-5}) \exp[(r-b)^{-1}] \quad (0 < r < b) \\ &= 0 \qquad\qquad\qquad\quad (b \leqslant r), \end{aligned} \tag{5.3}$$

where

$$\begin{aligned} B &= 6.767\,441\,448, \\ b &= 2.464\,918\,193. \end{aligned} \tag{5.4}$$

Just as for the dimensionless Lennard-Jones 12-6 potential, its minimum occurs at $2^{1/6}$ and has unit depth. Its zero-pressure stable crystal form is face centered cubic, in contrast to the hexagonal close packing produced by the Lennard-Jones potential.

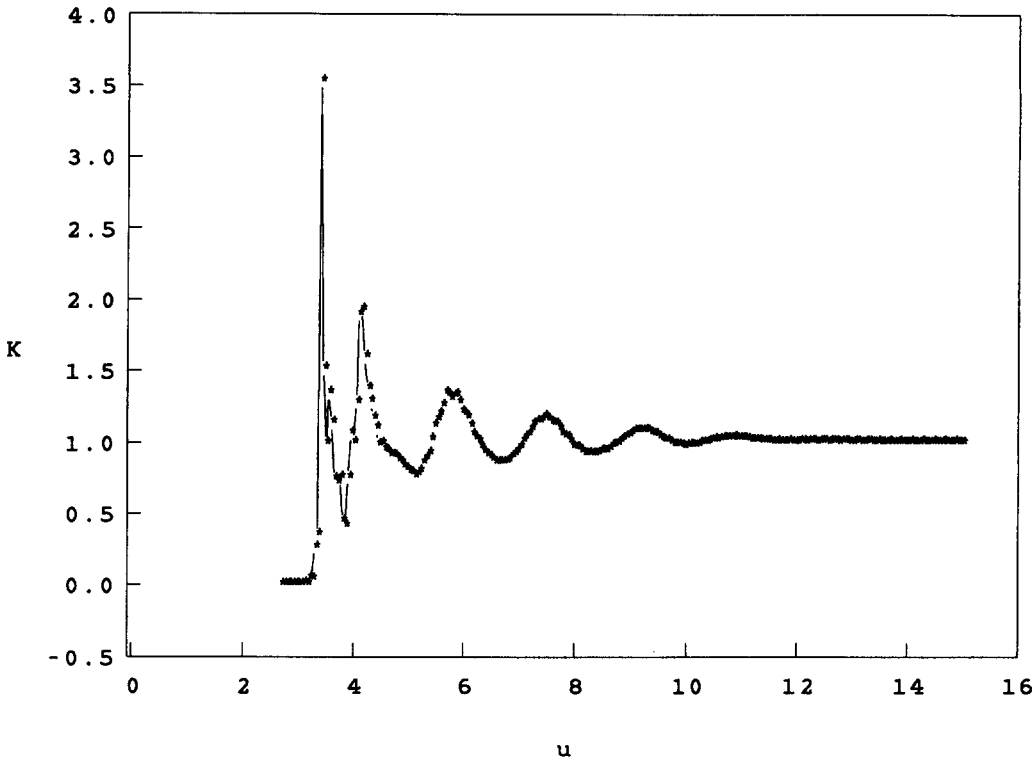

FIG. 9. $K(u)$ for the $\rho = 1.0$ Gaussian core model, obtained by inverting the BGY equation with the smoothed data of Fig. 8.

Figure 10 provides the amorphous-state $g(r)$ for the v_5 model from Ref. 23. The curve shown represents an average over 100 stable particle packings. These were obtained by steepest-descent quenching at equally spaced intervals during a molecular dynamics simulation of a slightly supercooled liquid. The system comprised 256 particles in a periodic unit cell at the density ($\rho = 1.066\,27$) of the zero-pressure, zero-temperature crystal. Notice that the local structure is significantly different from that displayed in Fig. 8 for the Gaussian core model. In order to solve the inverse problem for $K(u)$ over a substantial range in u, we were forced to extend the curve in Fig. 10 to fit smoothly onto the constant value unity at large r.

The result of the numerical inversion for the v_5 model is shown in Fig. 11. Although this again produces significant corrections to the superposition approximation, the result is

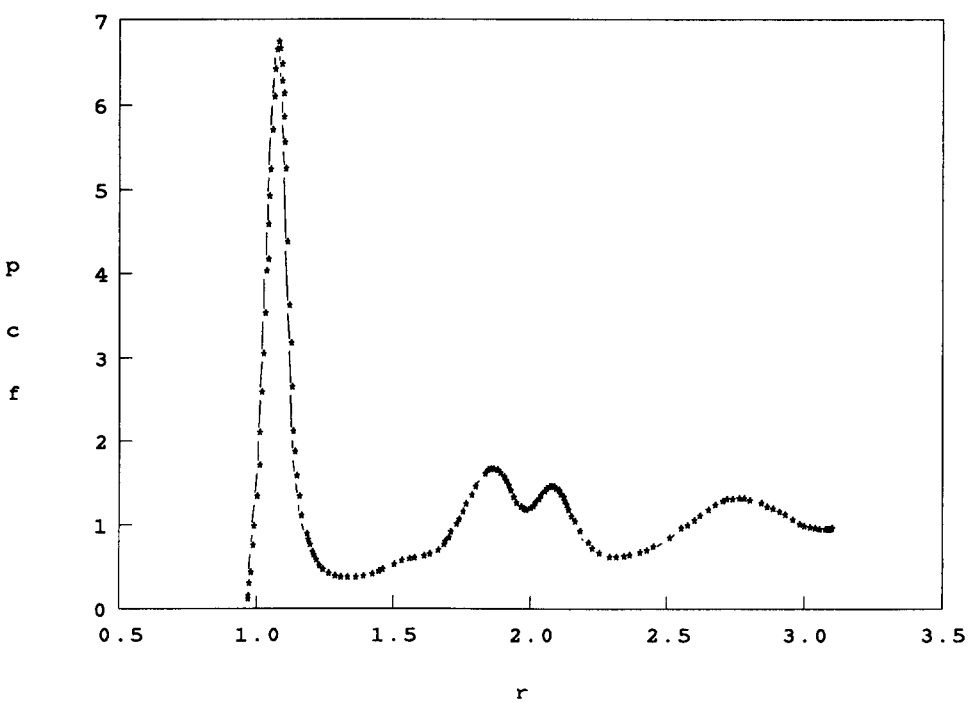

FIG. 10. Amorphous-state pair correlation function for the v_5 model, from Ref. 29.

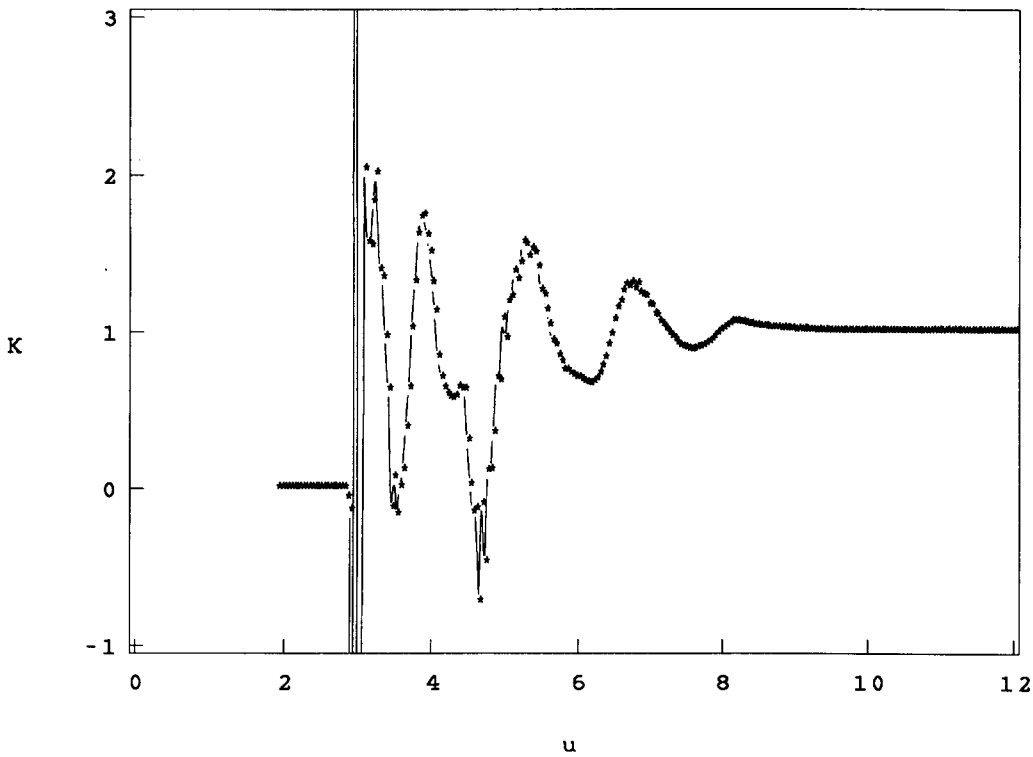

FIG. 11. $K(u)$ for the v_5 model, obtained by inverting the BGY equation with the molecular dynamics steepest descent quench pair correlation function of Fig. 10.

not satisfactory. The solution manifests numerical instability for $u \cong 3$ (with swings between -15 and $+18$), but even at the more significant larger u values K appears to become negative, a strictly forbidden feature. Nevertheless, it is perhaps significant that the range of K fluctuations about unity again is at least comparable to that of the input $g(r)$ fluctuations.

Other symmetrical combinations of r, s, and t beside the sum could have been considered in Eq. (5.1), such as $(r^2+s^2+t^2)^{1/2}$. It might be useful to explore some alternatives in the future, specifically to see if negative K values could be avoided.

VI. ASYMPTOTIC REGIME

The considerations in the preceding sections highlight the crucial role of the superposition defect function K for determining local order in amorphous solids with the BGY equation. We know on physical grounds that the nonrandomness of local order should die out quickly with increasing distance. In fact, a reasonable theoretical expectation is that if the interactions present have strictly finite range, then short-range order ought to decay exponentially with increasing distance. We can now uncover implicit conditions on K that assure such behavior.

For this purpose we now examine the large r_{12} asymptotic regime for the BGY equation (4.1). We shall suppose that pair potential $v(r)$ is negligibly small beyond some distance l, and that $r_{12} \gg$ l. Consequently, Eq. (4.1) simplifies to

$$-[\beta g(r_{12})]^{-1} g'(r_{12}) = \pi\rho r_{12}^{-2} \int_0^l dr_{13}\, v'(r_{13}) g(r_{13}) \int_{-r_{13}}^{r_{13}} dz (r_{12}+z) \times (r_{13}^2 - 2r_{12}z - z^2) g(r_{12}+z) K(r_{12}, r_{13}, r_{12}+z). \quad (6.1)$$

Here we have replaced variable r_{23} by $r_{12}+z$. In the large r_{12} limit under consideration the last two integrand factors, $g(r_{12}+z)$ and K, will both be close to unity. Hence, if we write

$$g(r) = 1 + h(r) \quad (6.2)$$

and also invoke the analogous expression (4.16) for K in terms of D, Eq. (6.1) leads to

$$-\beta^{-1} h'(r_{12}) \sim E(r_{12}) + \pi\rho r_{12}^{-2} \int_0^l dr_{13}\, v'(r_{13}) g(r_{13}) \times \int_{-r_{13}}^{r_{13}} dz (r_{12}+z)(r_{13}^2 - 2r_{12}z - z^2) h(r_{12}+z), \quad (6.3)$$

where E is the contribution of superposition corrections:

$$E(r_{12}) = \pi\rho r_{12}^{-2} \int_0^l dr_{13}\, v'(r_{13}) g(r_{13}) \int_{-r_{13}}^{r_{13}} dz (r_{12}+z) \times (r_{13}^2 - 2r_{12}z - z^2) D(r_{12}, r_{13}, r_{12}+z). \quad (6.4)$$

In deriving Eq. (6.3) we have disregarded terms that are nonlinear in the small quantities h and D, this being appropriate for the large r_{12} regime under consideration.

If $E(r_{12})$ were shorter ranged than $h(r_{12})$ then the asymptotic form of $h(r_{12})$ would be determined just by the homogeneous version of expression (6.3) obtained by dropping $E(r_{12})$. By substitution one verifies that then h would be

$$h(r_{12}) \sim r_{12}^{-1} \sum_j H_j \exp(ik_j r_{12}),$$

in direct analogy to the earlier hard-sphere expression (4.10). The k_j now are roots of

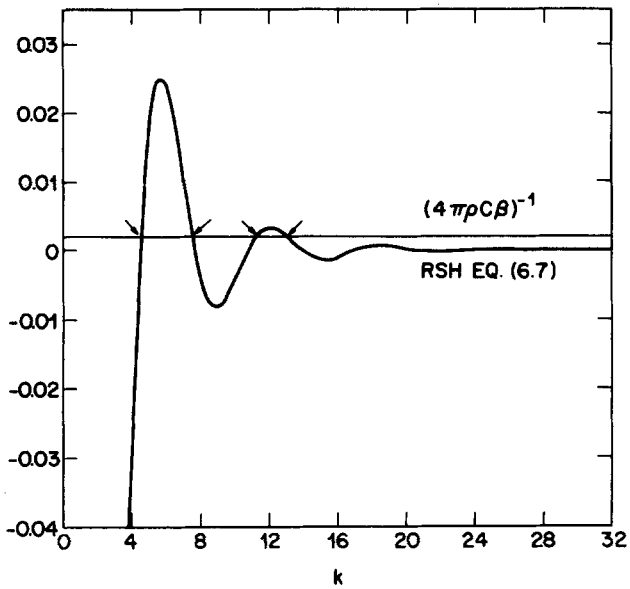

FIG. 12. Graphical solution of transcendental equation (6.7), for $\alpha = 50$, $4\pi\rho C\beta = 500$. Arrows locate positive real roots k_j; the pattern is repeated for negative real k.

$$-\beta^{-1} = 4\pi\rho k_j^{-3} \int_0^l dr_{13}\, v'(r_{13}) g(r_{13}) [k_j r_{13} \cos(k_j r_{13}) - \sin(k_j r_{13})]. \quad (6.5)$$

Even for non-hard-sphere interactions the $v'g$ combination in the integrand normally would have quite limited range. For purposes of illustrations we might assume, e.g.,

$$v'(r_{13})g(r_{13}) = -C(\alpha/\pi)^{1/2} \exp[-\alpha(r_{13}-1)^2]; \quad (6.6)$$

if α is sufficiently large the r_{13} integral can be extended to plus and minus infinity with negligible error, and then explicitly integrated to yield

$$(4\pi\rho C\beta)^{-1} = \{k_j \cos k_j - [1 + k_j^2/(2\alpha)] \sin k_j\} \times k_j^{-3} \exp(-k_j^2/4\alpha). \quad (6.7)$$

It is easy to see that the first factor $\{\cdots\}$ in the right member of Eq. (6.7) has an infinite number of real roots, and therefore so does the right member itself. These roots in turn are just those of the full equation at absolute zero, where the left member vanishes. A graphical analysis, Fig. 12, clearly shows how a rise in temperature above absolute zero causes pairs of roots to move off the real axis into the complex plane, leaving only a finite number of real roots near the origin. It seems unlikely to us that an alternative choice for $v'g$ would qualitatively change this scenario.

The real roots k_j appearing at low temperature are physically unacceptable, since the amorphous-state h must decay to zero more rapidly than r_{12}^{-1}. Evidently the only way that acceptable solutions can arise is that the corresponding coefficients H_j must vanish. This cannot be expected to occur unless the inhomogeneous function in Eq. (6.3) is suitably constrained, and that amounts to corresponding constraints (one for each real k_j) on the superposition correction K.

VII. CONCLUSIONS

This paper has presented the thesis that the Born–Green–Yvon integrodifferential equation in principle remains valid for supercooled liquids and amorphous solids, even in the limit of absolute zero temperature. In order to extract the experimentally relevant pair correlation function $g(r)$, however, the triplet correlation function $g^{(3)}$ needs to be specified. Differences in short-range order in low-temperature amorphous solids reflecting sample history arise from corresponding differences in $g^{(3)}$.

The approximation for $g^{(3)}$ most widely used in the equilibrium regime is the venerable Kirkwood superposition approximation. We have shown by several specific calculations (hard spheres, Gaussian core model at two densities, examination of the general large-distance case) that the superposition approximation leads to physically unacceptable predictions from the BGY equation.

One measure of the inappropriateness of the Kirkwood superposition approximation emerges from lattice enumerations, as originally pointed out by Alder.[34] Another indication is solution of the "inverse problem" posed in Sec. V, showing that subject to a special assumption about the functional form of corrections to superposition, those corrections must be large in magnitude and as long in range as $g(r)$ in order for the BGY equation to give the correct $g(r)$.

The weight of available evidence suggests that the role of the superposition correction K is not only to modify the magnitude of correlations intrinsic to the Kirkwood approximation, but also to change their qualitative nature for certain triplet configurations. The favorable (but not definitive) benefit of enhancing pentagonal structures (Sec. IV C) supports this viewpoint, but it is clearly necessary as well for K to disrupt the undamped pair correlations that tend to arise at low temperatures.

Finally, it seems obvious that detailed and exhaustive computer simulation studies of the triplet function $g^{(3)}$ for selected models of amorphous matter at absolute zero would be very beneficial. Such projects should be directed at determining how strongly $g^{(3)}$ depends on method of sample preparation, and at clarifying what specific details it must exhibit to satisfy the implicit criteria of Sec. IV that ensure damping of $g(r)$.

[1] Y. Waseda, *The Structure of Non-Crystalline Materials* (McGraw–Hill, New York, 1980).
[2] R. Zallen, *The Physics of Amorphous Solids* (Wiley, New York, 1983).
[3] *Glassy Metals II*, edited by H. Beck and H.-J. Güntherodt (Springer, Berlin, 1983).
[4] A. Rahman, M. J. Mandell, and J. P. McTague, J. Chem. Phys. **64**, 1564 (1976).
[5] H. R. Wendt and F. F. Abraham, Phys. Rev. Lett. **41**, 1244 (1978).
[6] F. H. Stillinger and T. A. Weber, J. Chem. Phys. **70**, 4879 (1979).
[7] S. Brawer, J. Chem. Phys. **72**, 4264 (1980).
[8] J. R. Fox and H. C. Andersen, J. Phys. Chem. **88**, 4019 (1984).
[9] M. H. Grabow and H. C. Andersen, Ann. N. Y. Acad. Sci. **484**, 96 (1986).
[10] T. L. Hill, *Statistical Mechanics* (McGraw–Hill, New York, 1956), Chap. 6.
[11] R. Kubo, *Statistical Mechanics* (North-Holland, Amsterdam, 1965), p. 109.
[12] F. H. Stillinger and T. A. Weber, Phys. Rev. A **25**, 978 (1982).

[13]F. H. Stillinger and T. A. Weber, Science **225**, 983 (1984).
[14]F. H. Stillinger and T. A. Weber, J. Phys. Chem. **87**, 2833 (1983).
[15]F. H. Stillinger, Phys. Rev. B **32**, 3134 (1985).
[16]F. H. Stillinger, J. Chem. Phys. **88**, 7818 (1988).
[17]G. Tammann and J. Starinkevitsch, Z. Phys. Chem. **85**, 573 (1913).
[18]I. Gutzow and I. Avramov, Thin Solid Films, **85**, 203 (1981).
[19]L. M. Brown and R. M. Mayer, Philos. Mag. **19**, 721 (1969).
[20]J. L. Brimhall, H. E. Kissinger, and L. A. Charlot, Radiat. Effects **77**, 213 (1983).
[21]O. Mishima, L. D. Calvert, and E. Whalley, Nature **310**, 393 (1984).
[22]F. H. Stillinger and T. A. Weber, J. Chem. Phys. **83**, 4767 (1985).
[23]F. H. Stillinger and R. A. LaViolette, Phys. Rev. B **34**, 5136 (1986).
[24]I. Z. Fisher, *Statistical Theory of Liquids*, translated by T. M. Switz (University of Chicago, Chicago, 1964), p. 140.
[25]F. H. Stillinger, Phys. Rev. **142**, 237 (1965).
[26]R. F. Kayser, J. B. Hubbard, and H. J. Raveche, Phys. Rev. B **24**, 51 (1981).
[27]L. R. Pratt, J. Chem. Phys. **87**, 1245 (1987).
[28]F. H. Stillinger and T. A. Weber, J. Chem. Phys. **80**, 4434 (1984).
[29]F. H. Stillinger and R. A. LaViolette, J. Chem. Phys. **83**, 6413 (1985).
[30]J. G. Kirkwood, J. Chem. Phys. **3**, 300 (1935).
[31]S. A. Rice and P. Gray, *The Statistical Mechanics of Simple Liquids* (Wiley–Interscience, New York, 1965), Sec. 2.7.
[32]E. Helfand and F. H. Stillinger, Chem. Phys. **37**, 2646 (1962).
[33]A. D. J. Haymet, S. A. Rice, and W. G. Madden, J. Chem. Phys. **74**, 3033 (1981).
[34]B. J. Alder, Phys. Rev. Lett. **12**, 317 (1964).
[35]A. Rahman, Phys. Rev. Lett. **12**, 575 (1964).
[36]W. J. McNeil, W. G. Madden, A. D. J. Haymet, and S. A. Rice, J. Chem. Phys. **78**, 388 (1983).
[37]J. A. Krumhansl and S. Wang, J. Chem. Phys. **56**, 2034 (1972); S. Wang and J. Krumhansl, *ibid.* **56**, 4287 (1972).
[38]H. J. Raveche, R. D. Mountain, and W. B. Streett, J. Chem. Phys. **57**, 4999 (1972).
[39]M. Tanaka and Y. Fukui, Prog. Theor. Phys. **53**, 1547 (1975).
[40]T. A. Weber and F. H. Stillinger, J. Chem. Phys. **81**, 5089 (1984).
[41]J. O. Hirschfelder, C. F. Curtiss, and R. B. Bird, *Molecular Theory Gases and Liquids* (Wiley, New York, 1954), pp. 1037–1039.
[42]Reference 24, p. 77.
[43]J. G. Kirkwood, E. K. Maun, and B. J. Alder, J. Chem. Phys. **18**, 1040 (1950).
[44]J. G. Kirkwood, V. A. Lewinson, and B. J. Alder, J. Chem. Phys. **20**, 929 (1952).
[45]D. Levesque, Physica **32**, 1985 (1966).
[46]D. A. Young and S. A. Rice, J. Chem. Phys. **47**, 4228 (1967).
[47]W. W. Lincoln, J. J. Kozak, and K. D. Luks, J. Chem. Phys. **62**, 2171 (1975).
[48]K. U. Co, J. J. Kozak, and K. D. Luks, J. Chem. Phys. **65**, 2327 (1976).
[49]K. U. Co, J. J. Kozak, and K. D. Luks, J. Chem. Phys. **66**, 581 (1977).
[50]Reference 10, p. 214.
[51]L. V. Woodcock, Ann. N. Y. Acad. Sci. **371**, 274 (1981).
[52]F. H. Stillinger, J. Chem. Phys. **65**, 3968 (1976).
[53]F. H. Stillinger, J. Chem. Phys. **70**, 4067 (1979).
[54]F. H. Stillinger, Phys. Rev. B **20**, 299 (1979).
[55]L. J. Root, F. H. Stillinger, and G. E. Washington, J. Chem. Phys. **88**, 7791 (1988).
[56]F. H. Stillinger and T. A. Weber, J. Chem. Phys. **68**, 3837 (1978); **70** 1074(E) (1979).
[57]F. H. Stillinger and T. A. Weber, J. Chem. Phys. **70**, 4879 (1979).
[58]F. H. Stillinger and T. A. Weber, Phys. Rev. B **22**, 3790 (1980).
[59]F. H. Stillinger and T. A. Weber, J. Chem. Phys. **74**, 4015 (1981).
[60]T. A. Weber and F. H. Stillinger, J. Chem. Phys. **74**, 4020 (1981).
[61]F. H. Stillinger and T. A. Weber, Phys. Rev. A **27**, 2642 (1983).
[62]K. U. Co, J. J. Kozak, and K. D. Luks, J. Chem. Phys. **66**, 4306 (1977).
[63]P. J. Steinhardt, D. R. Nelson, and M. Ronchetti, Phys. Rev. B **28**, 784 (1983).
[64]D. R. Nelson, Phys. Rev. B **28**, 5515 (1983).
[65]H. Jónsson and H. C. Andersen, Phys. Rev. Lett. **60**, 2295 (1988).